



Penetration profile of chloride ion in cracked reinforced concrete

Pa Pa Win*, Makiko Watanabe, Atsuhiko Machida

Department of Civil and Environmental Engineering, Saitama University, 255 Shimo-Okubo, Saitama, Saitama-Ken 338-8570, Japan

Received 9 April 2003; accepted 18 November 2003

Abstract

A detailed observation on the penetration profile of chloride ions through and around a crack in reinforced concrete structures was carried out. Electron probe microanalysis (EPMA) and colorimetric tests were conducted on cracked specimens, which were exposed to NaCl solution at a temperature of 20 °C and a humidity of 60% RH, after being conditioned in the same condition for 2 months. Research parameters included water to cement ratio (w/c), single and multicracks, exposed direction, crack width, NaCl solution concentration and cover thickness. Increasing w/c led to a higher ingress rate of Cl^- ions, not only from the exposed surface but also around the cracks. It was found that the penetration depth from the surface of the cracks was equal to or slightly higher than that from the exposed surface for higher w/c mixes of 0.45 and 0.65. The transportation of Cl^- ion was strongly influenced by the bulk movement of the solution inside the concrete.

© 2003 Elsevier Ltd. All rights reserved.

Keywords: EPMA; Crack; Chloride; Chloride ion concentration; Penetration depth

1. Introduction

Chloride-induced corrosion of reinforcing steel in concrete structures, such as bridge decks affected by deicing salt, and coastal and marine structures is a great problem everywhere. A considerable number of structures cease to function adequately. The estimation of the life span of reinforced concrete structures having cracks is influenced by their characteristics, such as crack width, crack length, etc., additional to the concrete properties and environmental exposure conditions as shown in Fig. 1.

Most previous research has been concerned with modeling the diffusion of chloride ions through uncracked concrete based on Fick's second law [5]. However, in practice, it is very common to have cracks in concrete structures in chloride ion environments. In that case, the transportation of chloride ions by water or moisture movement may take only a few hours to reach the steel, while penetration of ions through the uncracked concrete would take a longer time.

From Refs. [1,2], it was noted that the critical chloride content or threshold value, which has been established

recently, and that significant corrosion rates in noncarbonated concrete occur only at chloride contents of at least 1% of total chloride by cement weight. Almost all previous studies of effect of cracks on steel corrosion in cracked concrete were done by electrochemical methods [3].

This study was carried out on six series of small reinforced concrete beams (prisms) with variations on w/c,

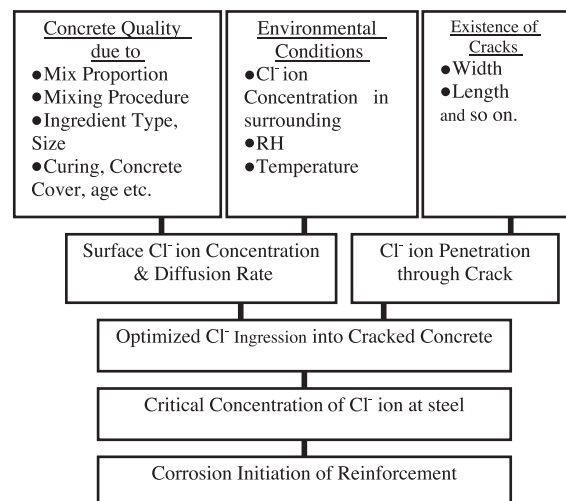


Fig. 1. Chloride-induced corrosion in cracked RC structures.

* Corresponding author. Tel.: +81-48-858-3550; fax: +81-48-858-7374.

E-mail address: papawin@mtr.civil.saitama-u.ac.jp (P.P. Win).

Table 1
Composition and property of cement

Density	3.16 g/cm ³
Specific surface area	3260 cm ² /g
Initial set (h:min)	2:15
Final set (h:min)	3:40
Soundness	Good
SO ₃	2.02%
IG loss	1.65%
Alkali content	0.54%
Cl content	0.012%
C ₃ S	52%
C ₂ S	22%
C ₃ A	9%
C ₄ AF	9%

single and multicroacks, exposed direction, crack width, NaCl solution concentration, and cover thickness. As a reference, specimens termed 45S28251, with w/c of 0.45, crack width of 0.2 mm, exposed to NaCl concentration of 8% by weight and with cover thickness of 25 mm were used.

2. Experimental program

2.1. Preparation of specimens and mix proportions

Six series, with 11 types of specimens, were prepared as shown in Table 3. Beam (Prism) specimens of 100×100×400 mm were reinforced with 2×Φ 10 mm plain bars for single-crack specimens and with deformed bars for multicrack specimens at the tension side. Cylinders of dimension Φ 100×200 mm were used for compressive strength testing.

Concrete ingredients used were ordinary Portland cement, with 5–12.3 mm crushed stone, fine aggregate, tap water and superplasticizer (SP) for w/c of 0.25. The SP used here was Rheobuild 8N, with a specific gravity of 1.05 g/cm³ at 20 °C and a Cl[−] content less than 0.01%. The composition and properties of the cement used are shown in Table 1.

The mix proportions were determined by following the process in Ref. [4]. The mix proportions, density and 28-day compressive strength are listed in Table 2. The specimens were sealed in a plastic bag for the first 28 days at 20 °C. After that, loading was applied to get the required crack width, which was measured using PI strain gauges

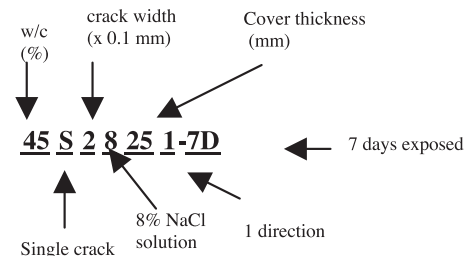


Fig. 2. Nomenclature of mix ID.

with 100-mm gauge length while loading, and crack gauge after the release of loading. Visible crack length ranged from 60 to 90 mm. A three-point bending test was applied to the single-crack specimens and a four-point bending test to the multicrack (mostly two cracks) specimens. The crack widths of the multicrack specimens could not be controlled to be uniform. The crack width of two cracks of the multicrack specimens in this study were 0.1 and 0.2 mm. The crack widths mentioned were the initial crack widths just before exposure, reduced with time, which could not be controlled in this experimental setup. The crack width was controlled in another experimental setup by using torque wrenches throughout the exposure time and will be presented in a separate paper. The single and multicrack series is used to observe the effect of adjacent cracks.

The specimens were epoxy-coated to prevent the penetration of Cl[−] ion from the sides that were not exposed. Therefore, coating was done depending upon the direction of flow of the NaCl solution. For each flow direction, the three layers of coating were applied to the unexposed surfaces by using primary, putty and epoxy as final coat. After all preparations, the specimens were kept in the control room, with temperature of 20 °C and RH of 60%, for precuring and waiting for exposure to NaCl solution.

The experimental setup was started at 3 months of concrete age in the control environment of a 20 °C and 60% RH room. Moisture contents just before exposure were found to be 75%, 74% and 65% for 0.25, 0.45 and 0.65 w/c samples, respectively. The specimens were laid in the solution trays of specified concentration for exposure time of 7 days and 1 month. Here, we carried out an exposure test with all series for 7 days (12 samples) and five samples, with mix IDs of 25S28251-1M, 45S28251-1M, 65S28251-1M, 45S23251-1M, 45S28451-1M, for 1 month. The notations for mix ID is explained in Fig. 2.

Table 2
Mix proportion and property of concrete

Number	Water to cement ratio	Cement (kg/m ³)	Water (kg/m ³)	Sand (kg/m ³)	Coarse aggregate (kg/m ³)	Aggregate volume (%)	Compressive strength (MPa)	SP, rehobuild	Density (kg/m ³)
1	0.25	720	180.0	614.40	880.50	57.1	81.04	0.80%	2356
2	0.45	424	190.8	768.00	941.60	67.3	45.04	–	2284
3	0.65	277	180.0	911.40	947.00	71.2	27.86	–	2238

In Table 3, the “1 direction” means that the Cl^- ions penetrated from the bottom surface of the prism specimens, supposing that the flow of solution, together with the Cl^- ions, took place mainly in the vertical direction. The “2 direction” means that the solution penetrated through the bottom and through one of the side surfaces of the beam specimen.

2.2. Testing details

The tests performed on the exposed specimens were electron probe microanalysis (EPMA) [6] for Cl^- ion concentration and penetration depth profile, and colorimetric tests with 0.1 M silver nitrate solution for the checking of the penetration depth of Cl^- ion and with 1.0% w/v phenolphthalein ethanol (90) solution (for $\text{pH} > 7.8$) for the carbonation depth. Colorimetric tests were done on separate adjacent cut specimens since spraying could not be carried out on the EPMA-tested specimens. The specimens were cut by using two different diamond blade cutters, without using water or oil to avoid the disturbance to Cl^- ions distribution inside while cutting. The cut specimen location inside the beam is shown in Fig. 3. The sizes of the specimens for EPMA were $< 76 \times 76 \times 18$ mm (length \times width \times thickness), from which, an array of approximately 400×400 numbers resulted for each of the elements mea-

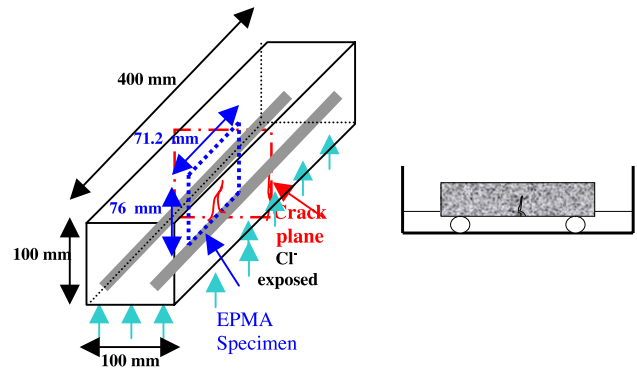


Fig. 3. Location of EPMA specimen in small RC beam.

sured, such as Cl^- , SO_3 , etc., which was used for further analysis. The concentration profiles of Na_2O , K_2O and SO_3 were also detected to get supporting information on the movement of Cl^- ions and carbonation, if any.

3. Result and discussion

After the start of experiment, bulk movement of solution containing Cl^- ions occurred along the crack and reached the crack tip within a very short time. Due to the continuous supply of solution and the initially low moisture content

Table 3
Series and type of specimens

Number	Mix ID	Water to cement ratio	Cracks	Crack width (mm)	NaCl solution concentration (%)	Cover thickness (mm)	Remark
Series (1) Water to cement ratio							
1	45S28251	0.45	Single	0.2	8%	25	1 direction
2	25S28251	0.25	Single	0.2	8%	25	
3	65S28251	0.65	Single	0.2	8%	25	
Series (2) Single and multicracks							
1	45S28251	0.45	Single	0.2	8%	25	1 direction
4	45M28251	0.45	Multi	0.1, 0.2	8%	25	
Series (3) Exposure direction							
1	45S28251	0.45	Single	0.2	8%	25	1 direction
5	45S28252	0.45	Single	0.2	8%	25	2 direction
Series (4) Crack width							
6	45S18251	0.45	Single	0.1	8%	25	1 direction
1	45S28251	0.45	Single	0.2	8%	25	
7	45S38251	0.45	Single	0.3	8%	25	
8	45S58251	0.45	Single	0.5	8%	25	
Series (5) NaCl concentration							
9	45S23251	0.45	Single	0.2	3%	25	1 direction
10	45S25251	0.45	Single	0.2	5%	25	
1	45S28251	0.45	Single	0.2	8%	25	
Series (6) Cover thickness							
11	45S28451	0.45	Single	0.2	8%	45	1 direction
1	45S28251	0.45	Single	0.2	8%	25	

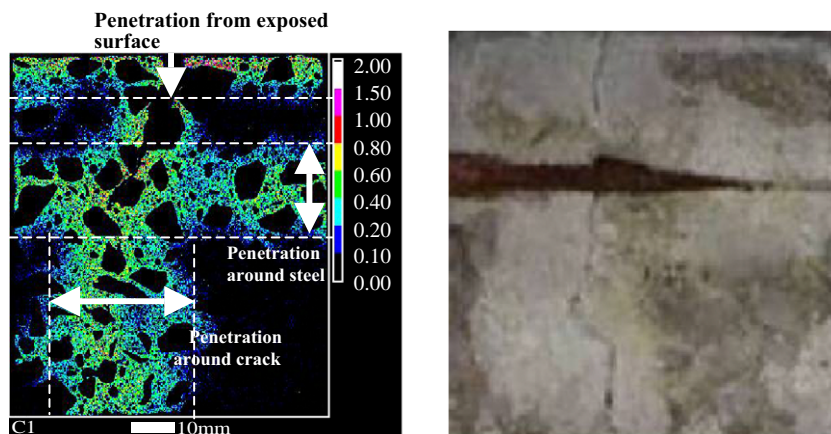


Fig. 4. EPMA and colorimetric test images of Cl^- ion distribution for 45S58251-7 days specimen.

inside the concrete, the moisture flow proceeded speedily to reach to the top of the beam of the specimens of 100-mm thickness within 3 h. Although the visible crack length from the side of specimens was only 60–90 mm, the NaCl solution penetrated to the top of the specimens and could be seen spreading on the top of the specimens, except on those specimens with shorter crack lengths, 0.25 w/c and 0.1-mm crack width, and a few with 4.5-cm cover thickness after 3 days of exposure to solution.

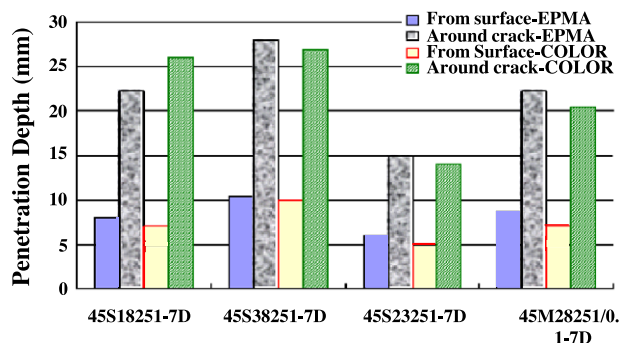


Fig. 5. Comparison of Cl^- ion penetration depth of some mixes for two types of tests.

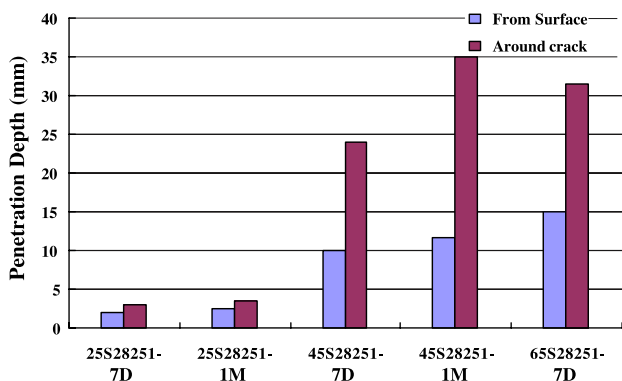


Fig. 6. Cl^- ion penetration depth of w/c series.

While the capillary suction flow of the bulk movement of the solution within the crack is taking place during exposure, a secondary movement of moisture containing Cl^- ions around the crack that is in perpendicular direction to the crack also took place. We also observed the horizontal flow along the steel once the penetrated solution moving along the crack reached the steel level. As the interface between steel and concrete is more porous due to bleeding, the flow in that direction is considerably fast, as shown in Fig. 4. Exceptions to this were the samples with a very low w/c of

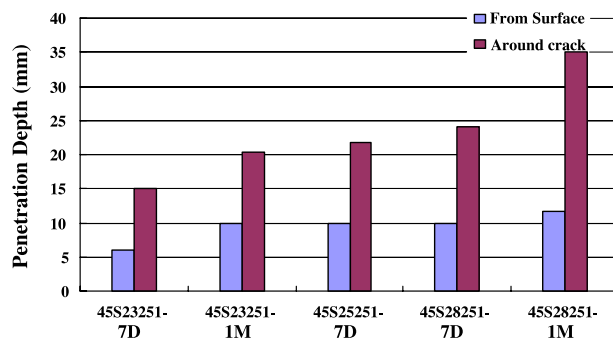


Fig. 7. Cl^- ion penetration depth of NaCl solution concentration series.

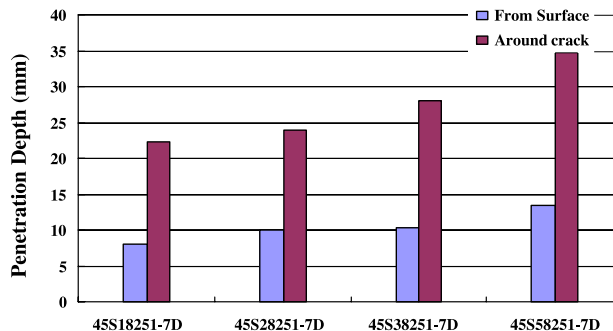


Fig. 8. Cl^- ion penetration depth of crack width series.

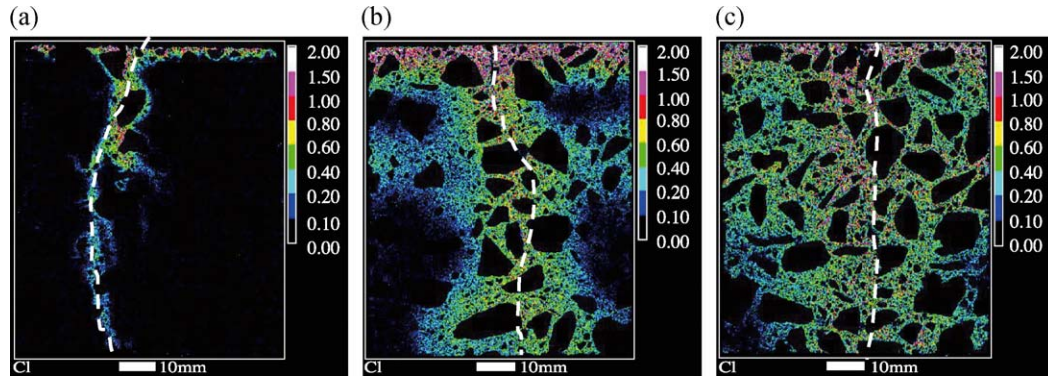


Fig. 9. EPMA images of Cl^- ion concentration for w/c ratio series (a) 0.25, (b) 0.45 and (c) 0.65, after 1 month of exposure.

0.25, which had no flow along the steel due to the denser structure.

3.1. Penetration depth of chloride ion

From EPMA test results, the “penetration depths” were measured from the grid lines on the EPMA images, where the clear profile could be seen for the concentration higher than 0.1% by weight of concrete. For colorimetric tests, measurements were carried out 3 days after the spraying of freshly cut specimens. The comparisons were made on the penetration depths of “penetration from exposed surface” and “penetration around crack” from EPMA and colorimet-

ric tests for some specimens because not all the colorimetric tested specimens showed a clear profile (see Fig. 4). Very similar results were found for those mixes tested by the EPMA and colorimetric tests, as shown in Fig. 5. Therefore, although the colorimetric test could not present concentration values, it is useful for preliminary viewing stages.

As shown in Figs. 6–8, it was found that the penetration depth around the crack (to both sides of crack) is slightly higher than twice of that from the exposed surface, except for mixes with low w/c of 0.25. It seems that the penetration from the surface of the crack (to only one side of crack) is similar in nature with the one from the exposed surface, and the slightly higher penetration might be due to the open

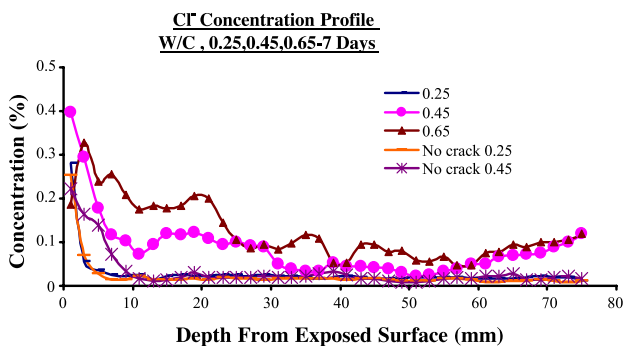


Fig. 10. Cl^- ion concentration profile of w/c series.

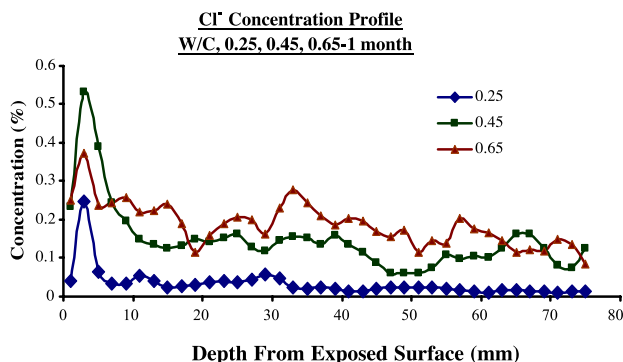


Fig. 11. Cl^- ion concentration profile of w/c series—1 month.

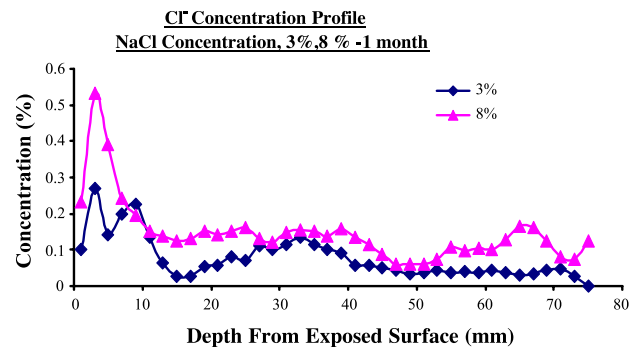


Fig. 12. Cl^- ion concentration profile of NaCl solution concentration series—1 month.

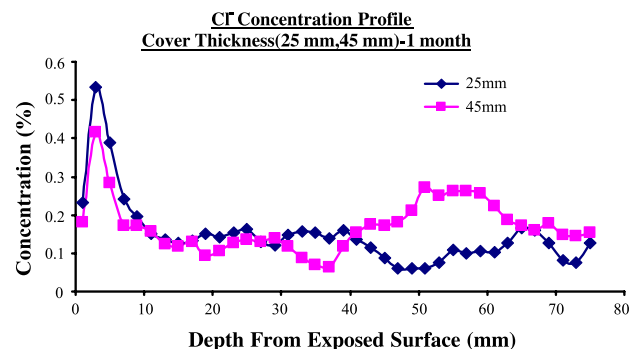
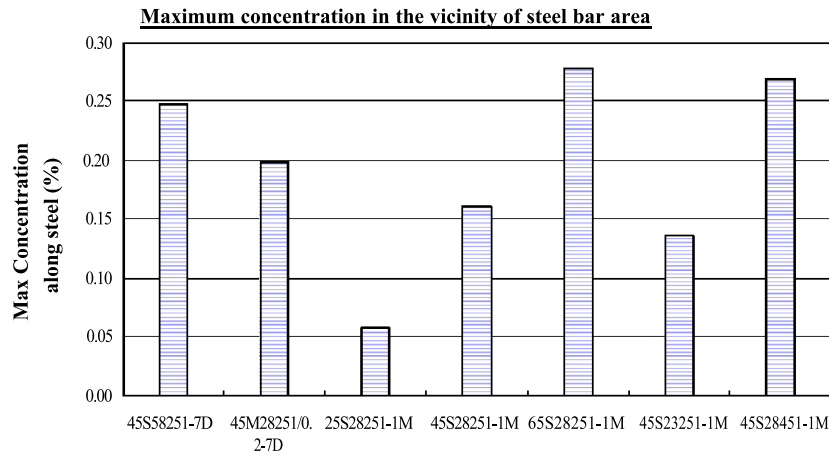
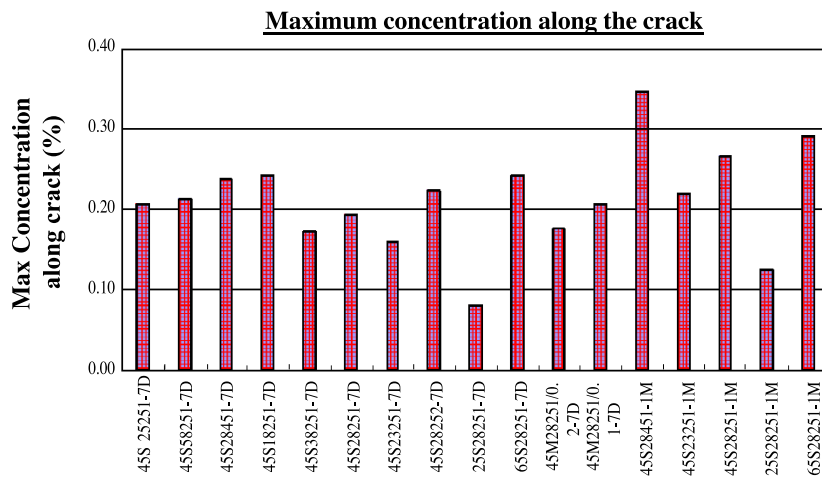


Fig. 13. Cl^- ion concentration profile of cover thickness series—1 month.

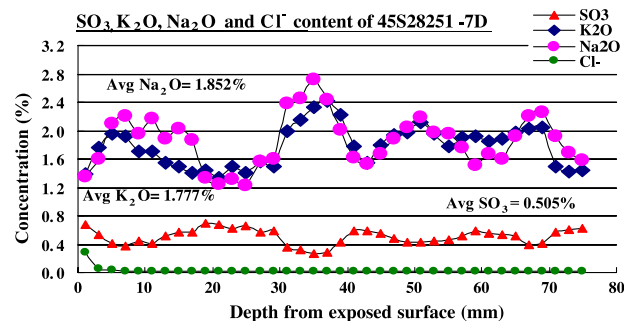
Fig. 14. Maximum Cl⁻ concentration around steel.Fig. 15. Maximum Cl⁻ concentration along crack.

pores and widened microcracks along the crack surface, which might increase the connectivity to interior pores. In addition, from Figs. 6–8, it can be seen that increase in w/c, being exposed to higher NaCl solution concentrations and wider crack widths led deeper penetration especially for a longer exposure time of 1 month. Therefore, it can be concluded that higher porosity, concentration gradient and larger crack widths could increase penetration rate.

The penetration depth in radial direction from the steel bar surface of the 45S58251-7D, 45M28251/0.2-7D, 45S28251-1M, 45S23251-1M, 45S28451-1M specimens was about 5 mm, which is less than the one from the exposed surface. Here, the 25S28251-1M, having no penetration along the steel, and 65S28251-1M specimens showed a wider spreading of penetrations from the exposed surface, around the crack and along the steel bar, and they were not distinguishable on the examined surface of the specimens, as shown in Fig. 9.

From Fig. 9, EPMA images for w/c ratio series after 1-month exposure showed an obvious increase in penetration

depth and concentration profile with an increase in w/c ratio. Undoubtedly, it can be seen that the quality of concrete has great influence on the penetration process, not only in uncracked concrete but also in cracked structures. At particular points near the exposed surface, the maximum Cl⁻ ion concentration was found to be 1.5–2% of percent weight of concrete in all of the 1-month exposed specimens.

Fig. 16. Concentration of Cl⁻, SO₃, K₂O and Na₂O.

For higher w/c of 0.45 and 0.65, it was found that, although the penetration depth from the crack surface is higher than the one from the exposed surface, the concentration values are lower. The reason for higher penetration depth might be due to small damages along the crack surface. However, the binding and adhering process of Cl^- ion along the penetrating path produced lower concentration values.

3.2. Concentration profile of Cl^- ion, SO_3 , K_2O and Na_2O

All the concentration data presented here are in percent weight of concrete which resulted from the EPMA test. The concentration value at a particular depth means an average concentration within 2-mm depth, each on a fixed area of 76×71.2 mm (depth \times width). As expected, from the w/c series and NaCl solution concentration series, a clear trend is found that the higher the w/c ratio and NaCl solution concentration, the higher the concentration of Cl^- ions over the depth of specimen due to having cracks (see Figs. 10–12). The capillary flow of the NaCl solution in the crack passed through the steel level, and due to the continuous availability of the solution in both cases of 25- and 45-mm cover thicknesses, the effect of cover thickness on concentration profile was not clear in this experiment, as shown in Fig. 13.

Except the 0.5-mm crack width specimen which showed relatively higher penetration results, all others from the crack width series showed more or less similar distribution of concentration, regardless of crack width.

The maximum Cl^- concentrations around the steel of seven specimens were observed and are shown in Fig. 14. In this study, although the maximum concentration of Cl^- ion around the steel bar of some specimens exceeded the optimum limit of 0.4% of free chloride by weight of cement (which is equivalent to 0.195% for 0.45 w/c and 0.128% for 0.65 w/c by weight of concrete in this study, assuming a free to bound chloride ratio of 0.6 [2]), the corrosion initiation was not seen. Probably, it might be due to the insufficient oxygen supply to the steel area and the very short exposure time.

Fig. 15 shows the maximum Cl^- ion concentration along the surface of the crack, which is the average value observed within the 2-mm distance around the crack. Up to 1-month exposure time, the concentrations of SO_3 , K_2O and Na_2O were not affected by Cl^- ion movement in the cracked specimens. The origin of SO_3 is the cement. Although there is some alkali content in the cement, the K_2O and Na_2O are mainly found from aggregates in this concrete (see Fig. 16).

4. Conclusions

In this study, we used a series of cracked reinforced concrete specimens, which were sealed and cured in plastic bags for the first 28 days, and were then conditioned in the controlled room at a temperature of 20 °C and 60% RH for about 2 months. Therefore, specimens were about 3 months of concrete age at the time of exposure to NaCl solution and were partially in dry condition. From this research, we found that the reinforced concrete specimens having cracks showed rapid penetration of Cl^- ion, which finally reached the steel, and penetration along the steel also occurred. Specimens with low w/c ratio of 0.25 showed lower concentration profile and penetration depth both from exposed surface and around the crack compared with w/c ratios of 0.45 and 0.65. No penetration along the steel was observed for specimens with w/c of 0.25. The increase in w/c led to a higher ingress rate of Cl^- ions, not only from the exposed surface, but also around the crack. In general, the penetration depth from the surface of the crack is equal to or slightly higher than that from exposed surface in higher w/c mixes of 0.45 and 0.65. From this study, the movement of Cl^- ions along with the bulk solution movement through the crack and within the concrete can occur when the capillary suction is taking place. This fact has great influence, rather than diffusion mechanism, and should not be ignored for real structures. There might have a critical limit of free ion movement due to flow of bulk solution and followed by diffusion mechanism after the steady stage of moisture flow.

References

- [1] R.B. Polder, Laboratory testing of five concrete types for durability in a marine environment, in: C.L. Page, P.B. Bamforth, J.W. Figg (Eds.), *Corrosion of Reinforcement in Concrete Construction*, The Royal Society of Chemistry, Cambridge, 1996, pp. 115–123.
- [2] T.U. Mohammed, T. Yamaji, H. Hamada, Chloride diffusion, microstructure, and mineralogy of concrete after 15 years of exposure in tidal environment, *ACI Mater. J.* 99 (3) (2002) 256–263.
- [3] K. Suzuki, Y. Ohno, S. Praparntanatorn, H. Tamura, Mechanism of steel corrosion in cracked concrete, in: C.L. Page, K.W.J. Treadaway, P.B. Bamforth (Eds.), *Corrosion of Reinforcement in Concrete*, Elsevier Applied Science, London, 1996, pp. 19–28.
- [4] *Concrete Manual*, 8th ed., U.S. Department of the Interior, Bureau of Reclamation, 1975.
- [5] E.P. Nielsen, M.R. Geiker, Chloride diffusion in partially saturated cementitious materials, *Cem. Concr. Res.* 33 (1) (2003) 133–138.
- [6] P.E.J. Flewitt, R.K. Wild, *Physical Methods for Materials Characterisation*, IOP Publishing, London, 1994.